Electronic Supplementary Information (ESI)

Enhancing photocatalytic performance of F-doped TiO_2 through the integration of small amounts of a quinoline-based covalent triazine framework

Alicia Moya[a], Miguel Sánchez-Fuente[a], Marta Linde[a], Víctor Cepa-López[a], Isabel del Hierro[b,c], Miguel Díaz-Sánchez*[b], Santiago Gómez-Ruiz*[b,c], Rubén Mas-Ballesté*[a,d]

[a]*Departamento de Química Inorgánica, Facultad de Ciencias, Calle Francisco Tomás y Valiente, 7, Universidad Autónoma de Madrid, Ciudad Universitaria de Cantoblanco, 28049, Madrid, Spain*

[b]*COMET-NANO Group, Departamento de Biología y Geología, Física y Química Inorgánica, E.S.C.E.T., Universidad Rey Juan Carlos, Calle Tulipán s/n, E-28933, Móstoles, Madrid, Spain*

[c]*Instituto de Investigación de Tecnologías para la Sostenibilidad. Universidad Rey Juan Carlos. C/ Tulipán s/n. 28933 Móstoles. Madrid. Spain.*

[d]*Institute for Advanced Research in Chemical Sciences (IAdChem), Facultad de Ciencias, Calle Francisco Tomás y Valiente, 7, Universidad Autónoma de Madrid, Ciudad Universitaria de Cantoblanco, 28049, Madrid, Spain*

Correspondence: miguel.diaz@urjc.es, santiago.gomez@urjc.es and ruben.mas@uam.es

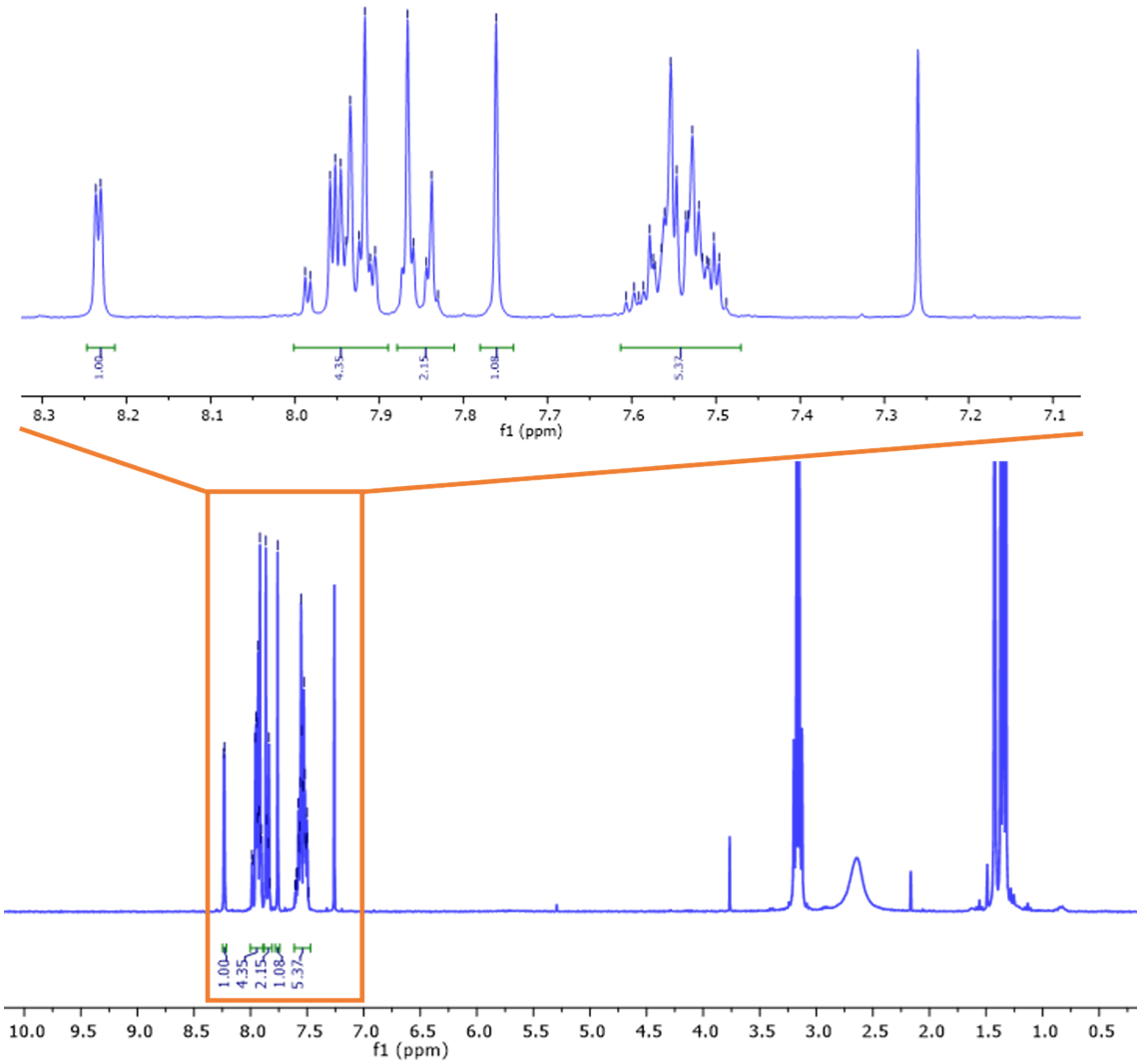

Fig. S1. ^{1}H-NMR spectra of the obtained product **Quin-I**.

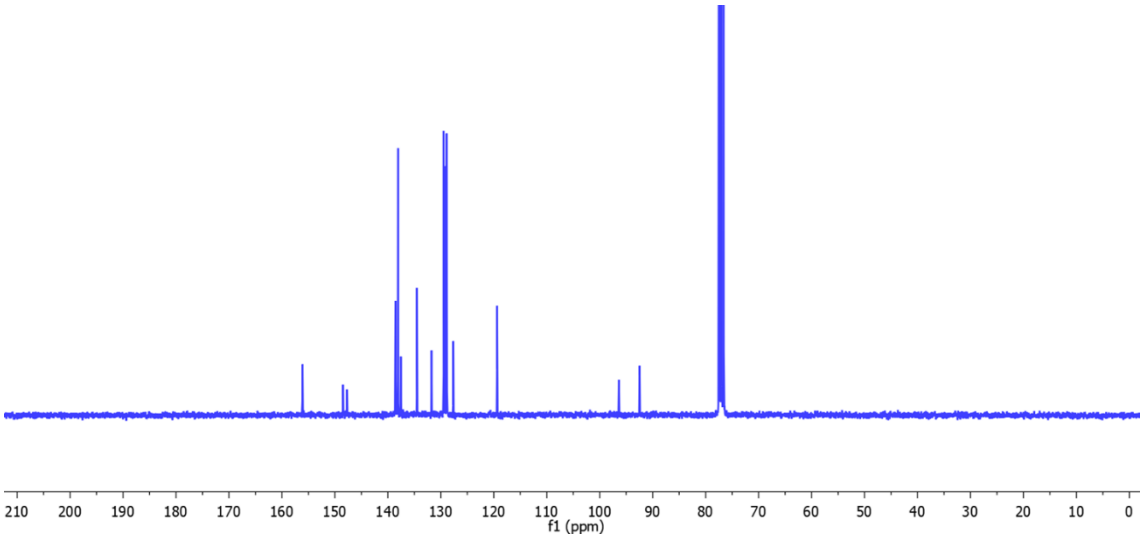

Fig. S2. ^{13}C-NMR spectra of the obtained product **Quin-I**.

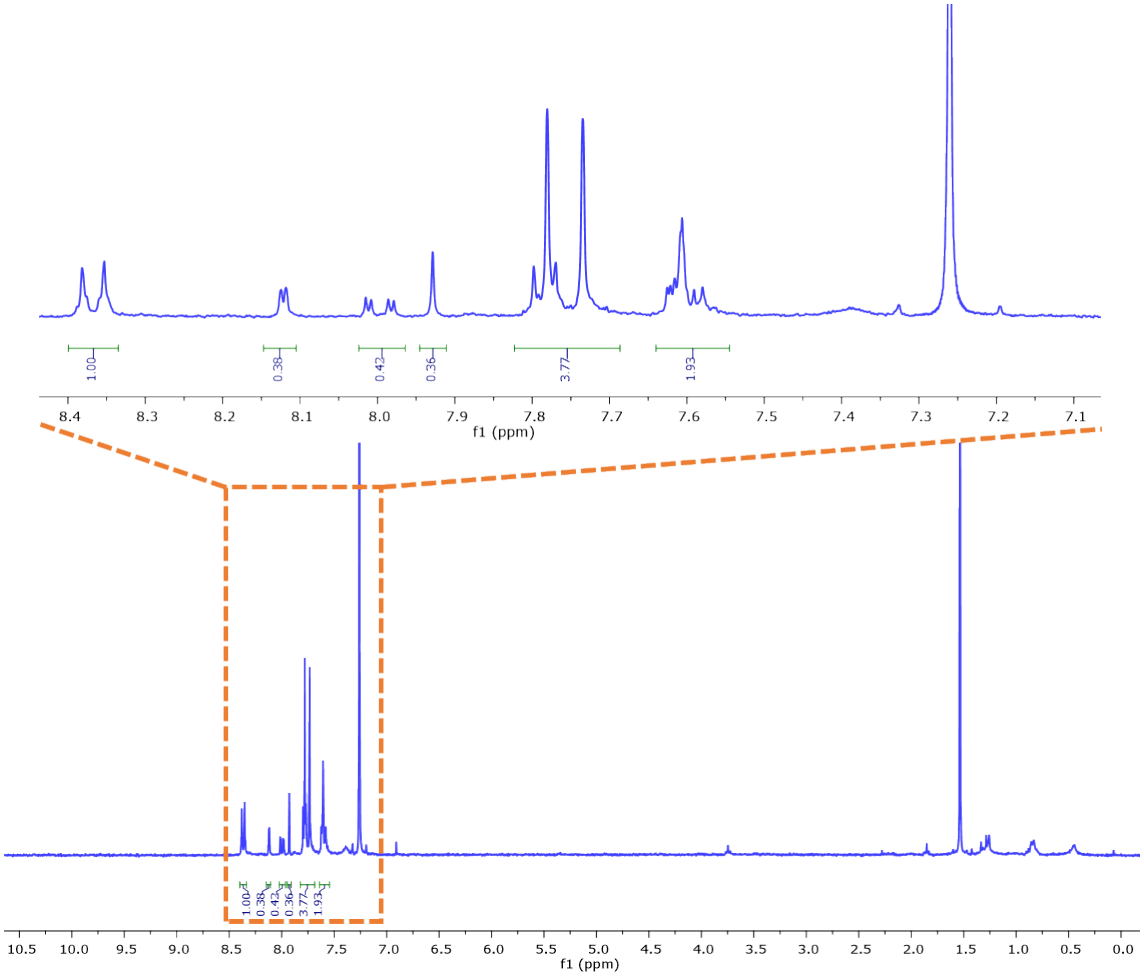

Fig. S3. ^{1}H-NMR spectra of the obtained product **Quin-CN**.

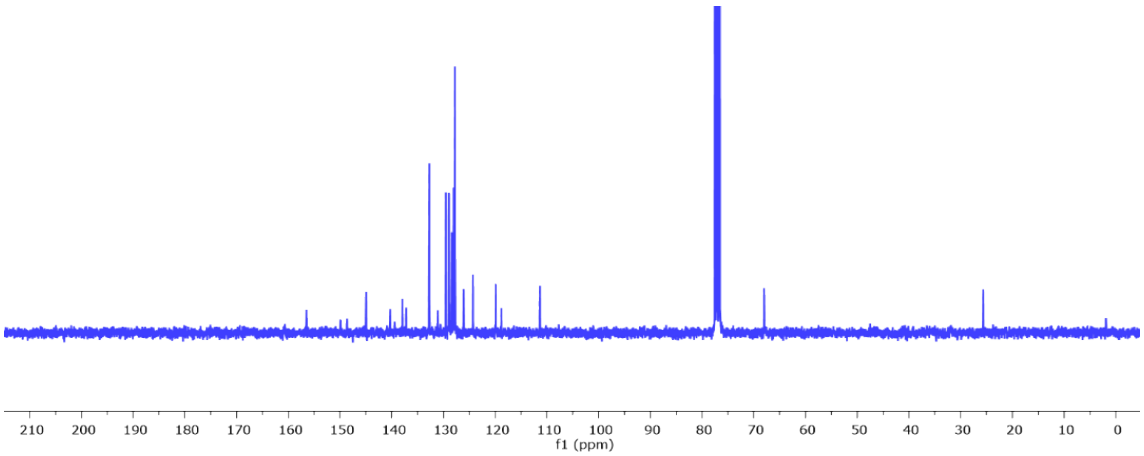

Fig. S4. ^{13}C-NMR spectra of the obtained product **Quin-CN**.

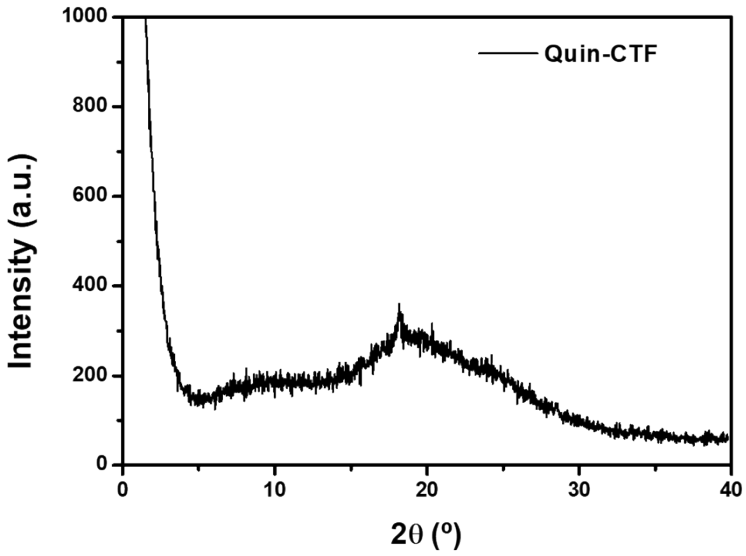

Fig. S5. XRD pattern of **Quin-CTF** material.

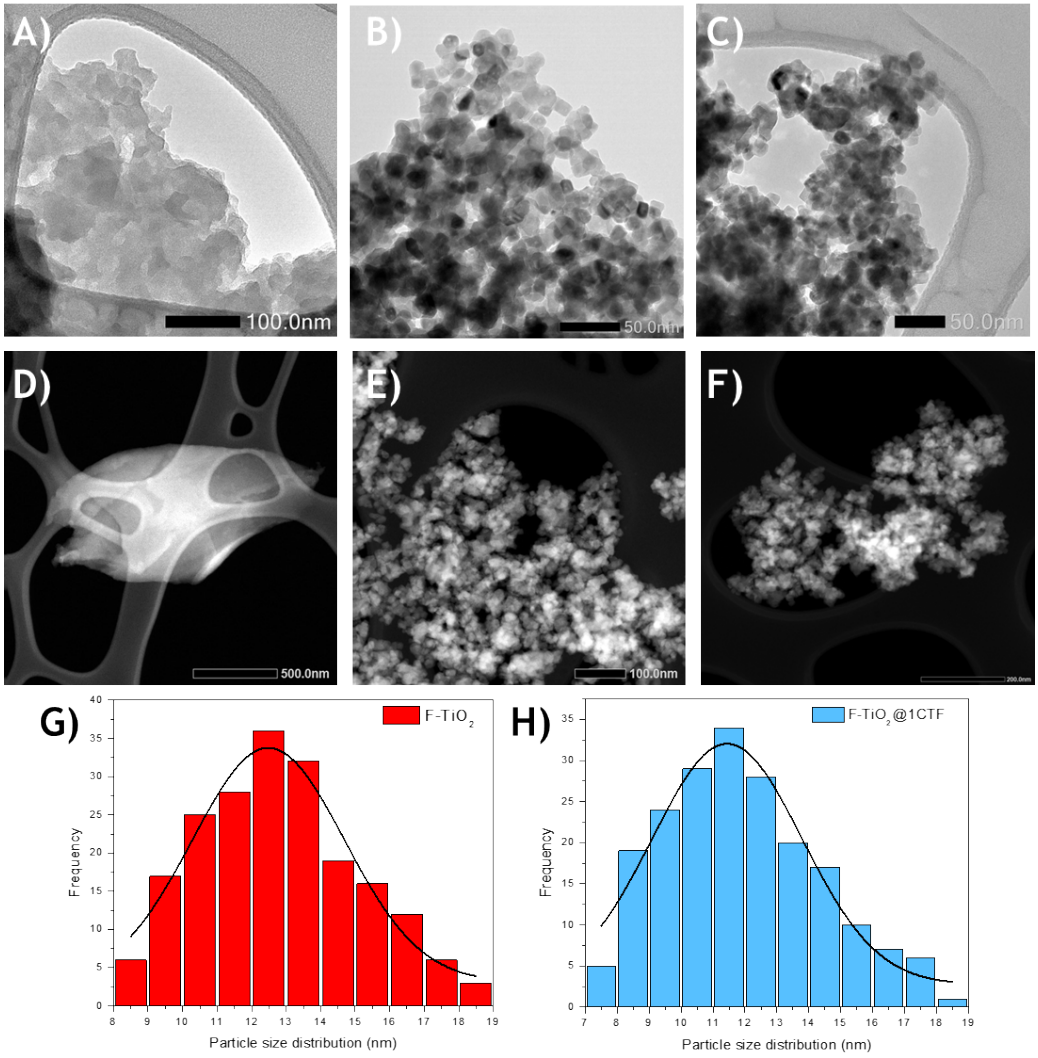

Fig. S6. A-C) TEM and D-F) HAAD-TEM images of **Quin-CTF** (left), **F-TiO$_2$** (middle) and **F-TiO$_2$@1CTF** (right) materials. Particle size distribution of G) **F-TiO$_2$** and F) **F-TiO$_2$@1CTF** materials measured from HRTEM images.

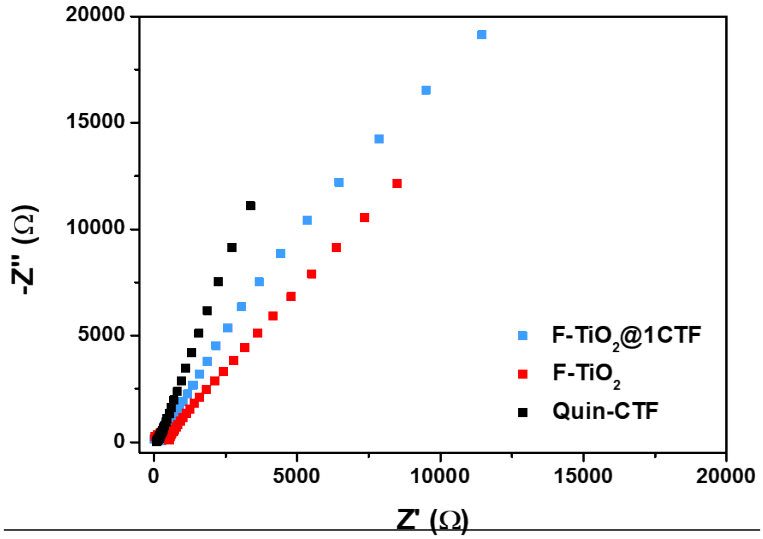

Fig. S7. Electrochemical impedance spectra of **F-TiO$_2$, F-TiO$_2$@1CTF** and **Quin-CTF** in Na_2SO_4 0.2 M vs Ag/AgCl (3M KCl): Nyquist plots obtained without applying bias.

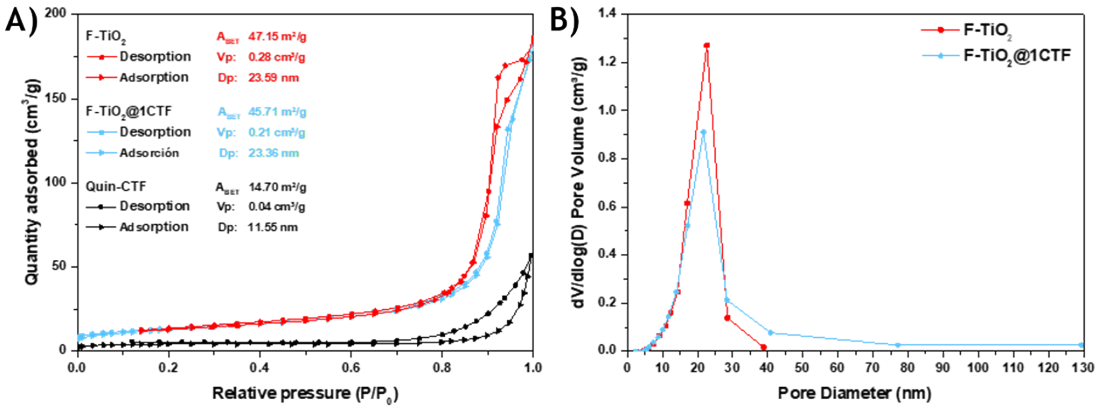

Fig. S8. A) Nitrogen adsorption-desorption isotherms of **F-TiO$_2$, F-TiO$_2$@1CTF** and **Quin-CTF** materials and B) BJH pore size distribution of **F-TiO$_2$** and **F-TiO$_2$@1CTF** systems.

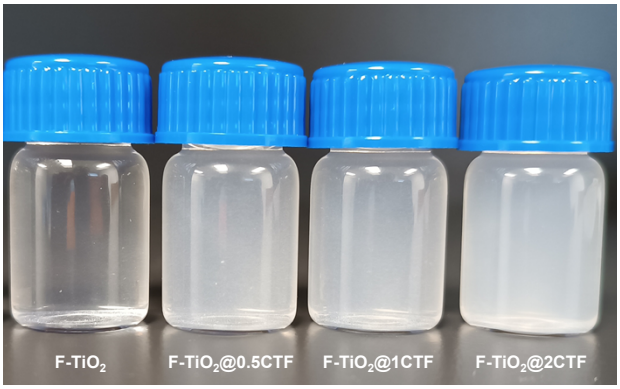

Fig. S9. Dispersion by sonication of the **F-TiO$_2$** and hybrid materials at a rate of 1 mg in 10 mL of ultrapure H_2O.

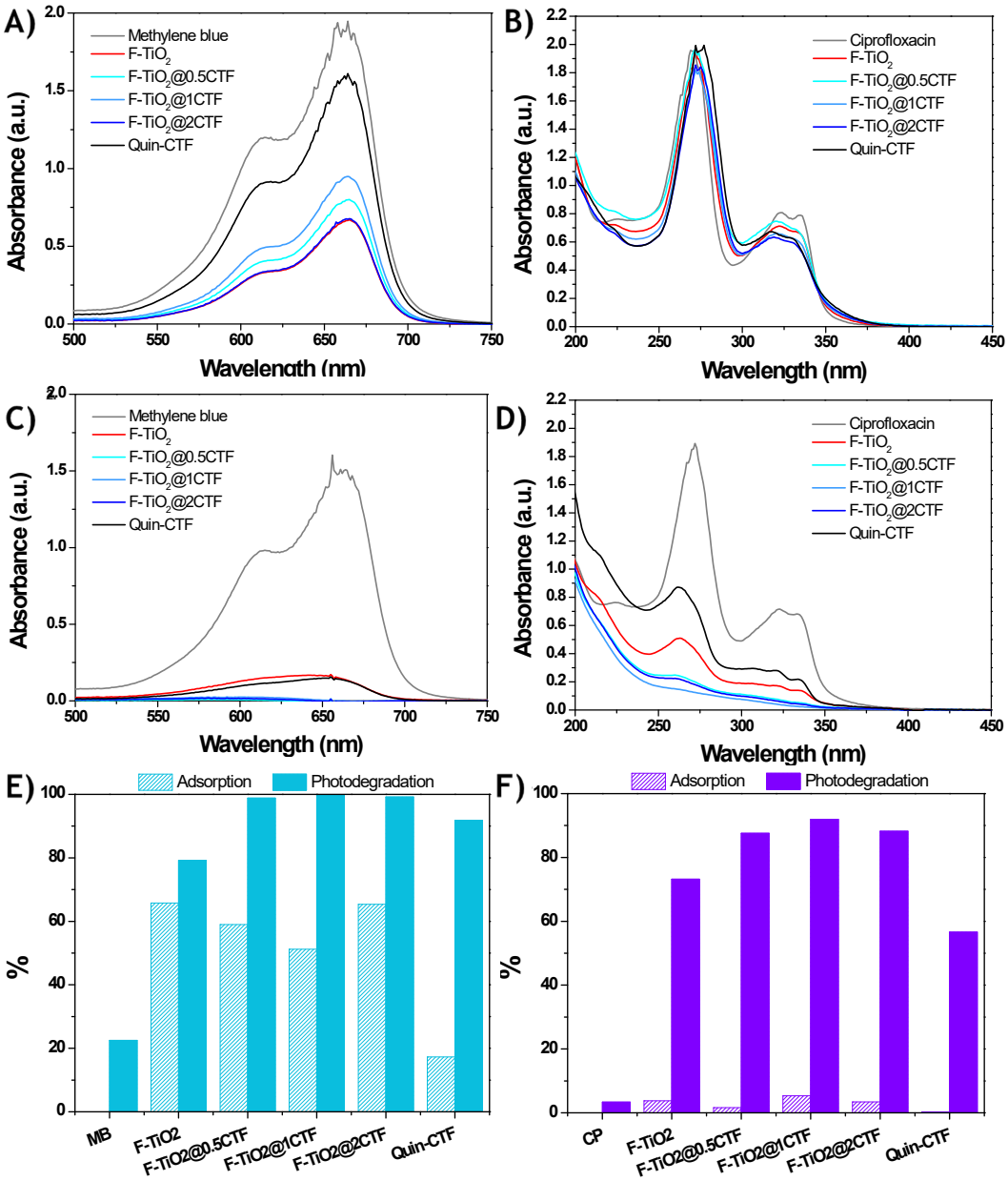

Fig. S10. UV-visible absorption spectra of the adsorption tests (1h in dark condition) for A) MB and B) CP. UV-visible absorption spectra of the photodegradation tests under 385 nm irradiation of C) MB (50 minutes) and D) CP (30 minutes). Bar diagrams with the % adsorbed (dashed bars) and photodegraded (solid bars) of E) MB and F) CP pollutants.

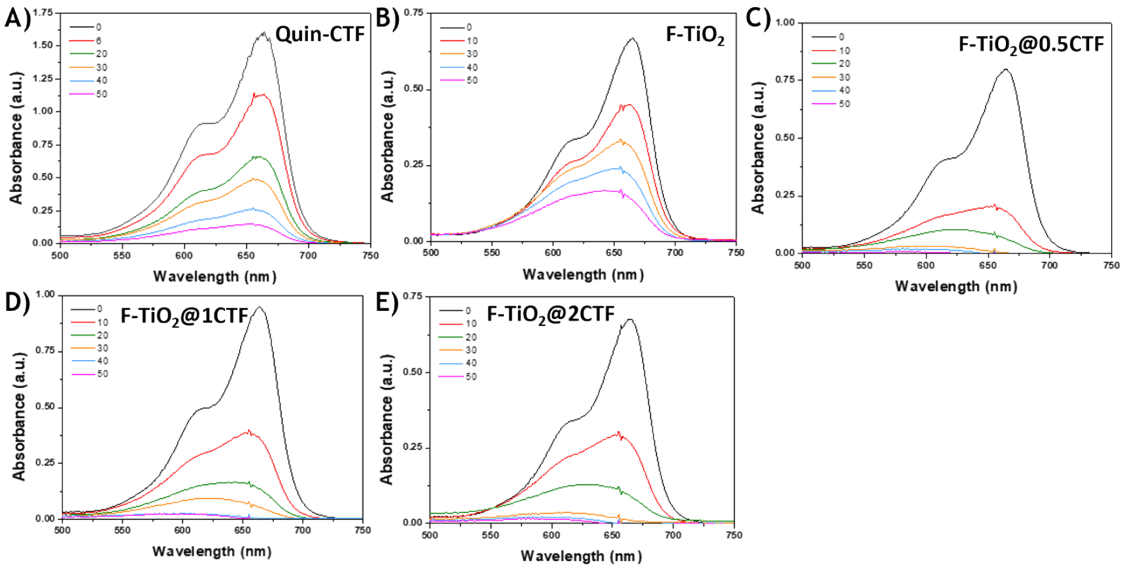

Fig. S11. A-E) UV-visible absorption spectra of the kinetic tests for the photodegradation of MB (50 minutes of 385 nm irradiation) using all photocatalysts of this study.

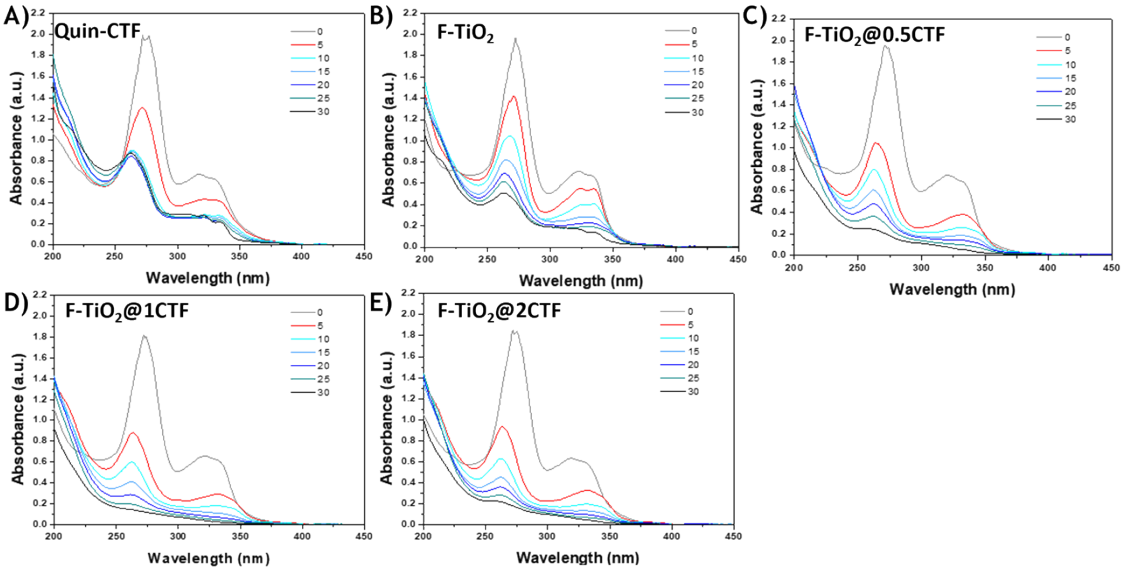

Fig. S12. A-E) UV-visible absorption spectra of the kinetic tests for the photodegradation of CP (30 minutes of 385 nm irradiation) using all photocatalysts of this study.

Table S1. Comparison of TiO_2-Based Photocatalysts for MB Degradation

Material	Rate Constant (k, min^{-1})	Mass ratio MB/PC	Ref.
P25	0.011	0.025	[1]
P25	0.025	0.01	[2]
P25	0.055	0.02	[3]
TiO_2	0.017	0.1	[4]
TiO_2	0.013	0.03	[5]
TiO_2	0.046	0.012	[6]
TiO_2	0.022	0.025	[1]
TiO_2	0.01	0.003	[7]
TiO_2/Graphene Oxide	0.025	0.05	[8]
TiO_2/Graphene Oxide	0.015	0.03	[5]
TiO_2/Activated carbon	0.029	0.03	[5]
TiO_2/CNT	0.009	-	[9]
TiO_2/CNT	0.008	0.02	[10]
F-TiO_2	0.025	0.04	This work
Quin-CTF	0.045	0.04	This work
F-TiO_2@1CTF	0.077	0.04	This work

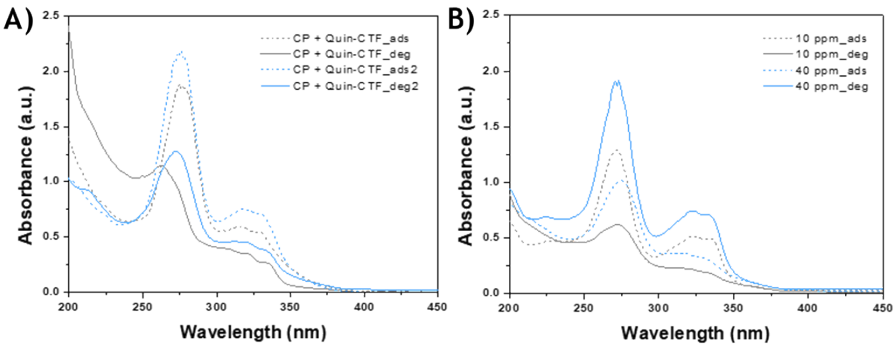

Fig. S13. UV-visible absorption spectra using **Quin-CTF** as photocatalytic material for the photodegradation of CP. A) Essay on recyclability of **Quin-CTF** material and B) Photodegradation test using 10 and 40 ppm of CP.

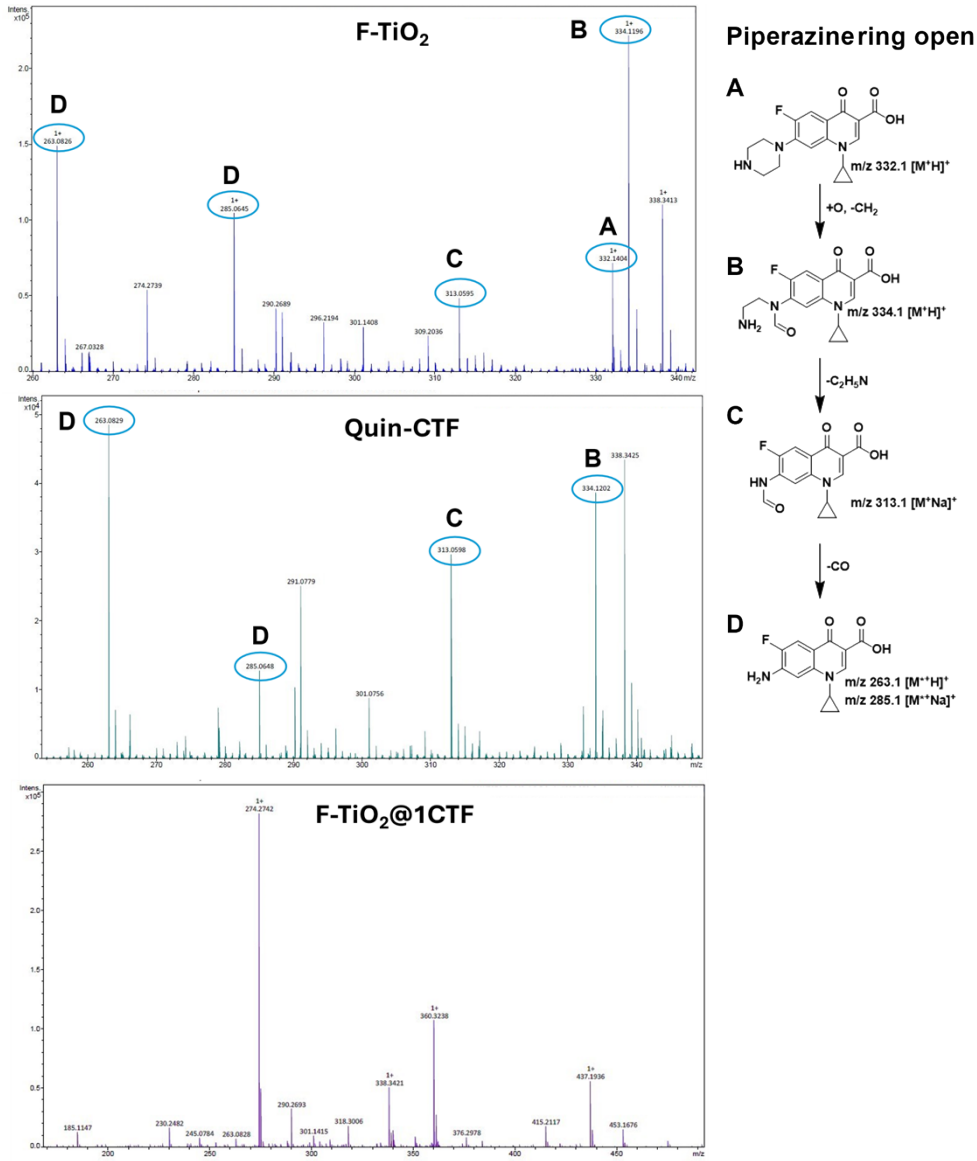

Fig. S14. MS/MS spectra of ciprofloxacin fragments obtained after 30 minutes of photocatalytic process using **F-TiO$_2$** (upper spectra), **Quin-CTF** (medium spectra) and **F-TiO$_2$@1CTF** (bottom spectra) as photocatalysts. Schematic of ciprofloxacin degradation through the piperazine ring open pathway indicating the CP fragments and their m/z signals.

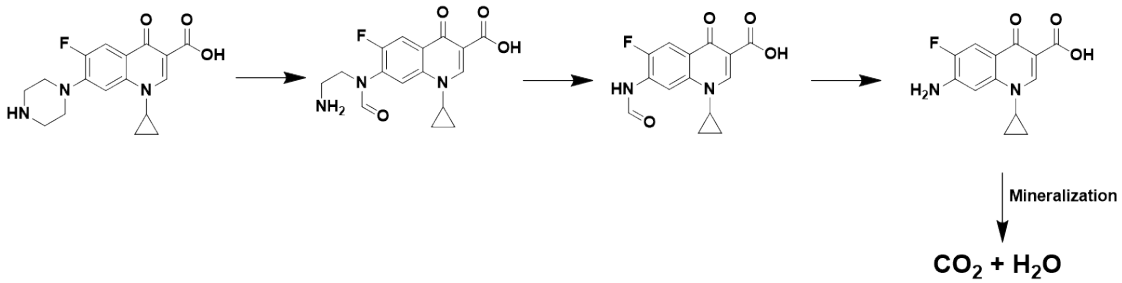

Fig. S15. Scheme of the reaction pathway for the ciprofloxacin photodegradation reaction.

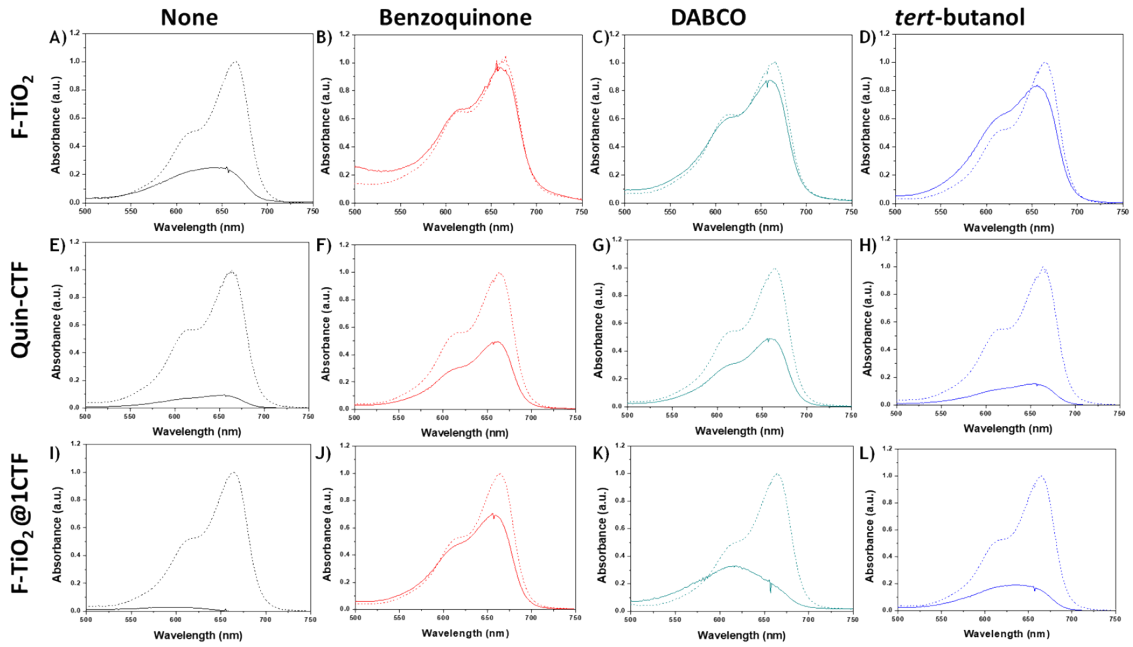

Fig. S16. UV-visible absorption spectra of MB of the scavenger essays of A-D) **F-TiO$_2$**, E-H) **Quin-CTF** and I-L) **F-TiO$_2$@1CTF**. Black, red, green and blue spectra correspond to experiments without scavengers and with benzoquinone, DABCO and tert-butanol, respectively. Dashed lines correspond to the absorption spectra after adsorption in dark conditions and solid lines to the absorption spectra after photodegradation experiments.

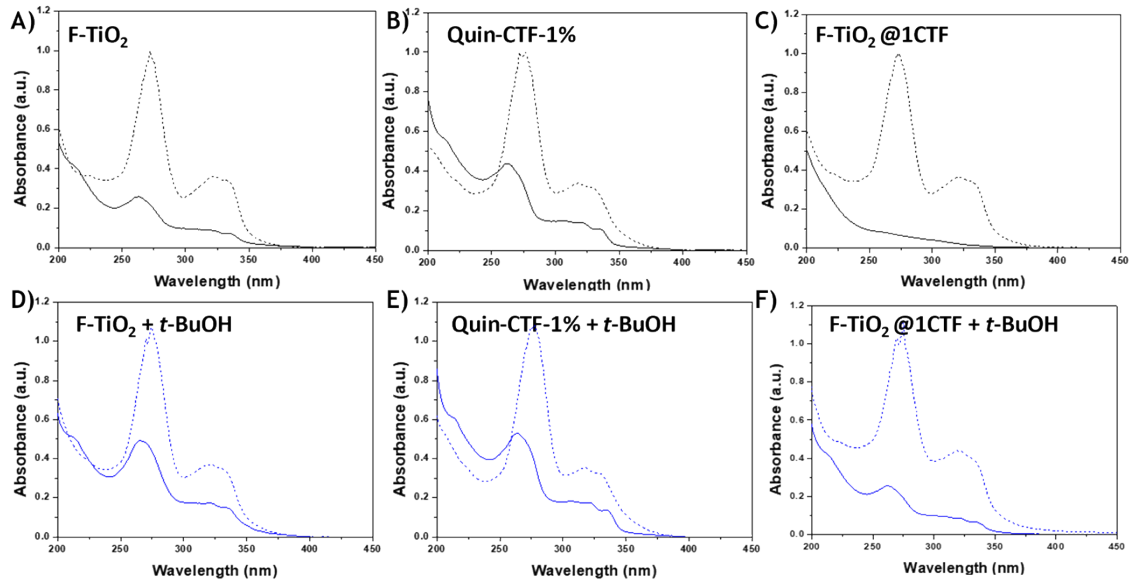

Fig. S17. UV-visible absorption spectra of CP without (A-C) and with (D-F) tert-butanol (*t*-BuOH) as scavenger of hydroxyl radicals for the **F-TiO$_2$, Quin-CTF** and **F-TiO$_2$@1CTF**. Dashed spectra corresponds to initial spectra after 1h of adsorption in dark conditions and solid spectra corresponds to the absorption spectra after 30 minutes of photodegradation.

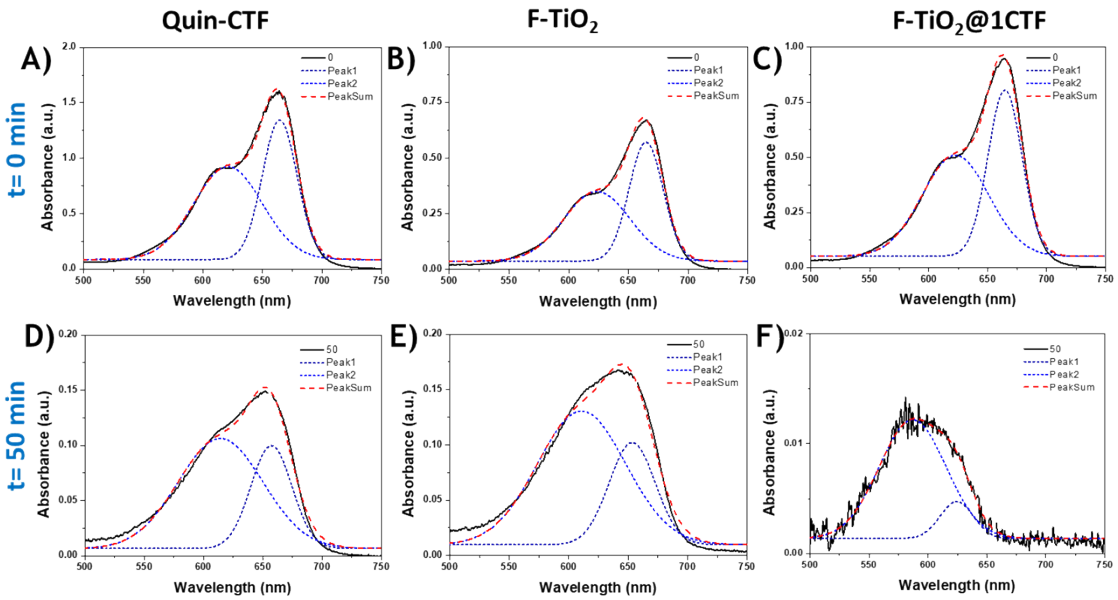

Fig. S18. Methylene blue spectral deconvolution analysis at A-C) t=0 and D-F) t=50 minutes (bottom spectra) of photocatalytic reaction.

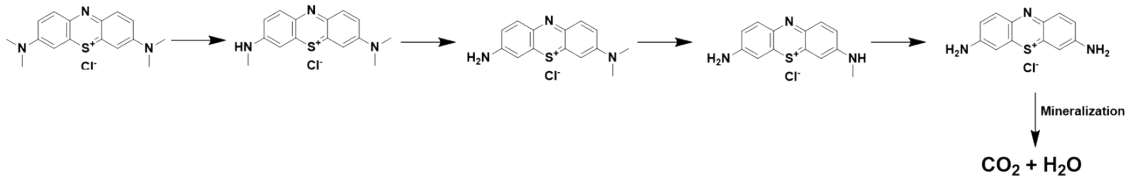

Fig. S19. Scheme of the reaction pathway for the methylene blue photodegradation reaction.

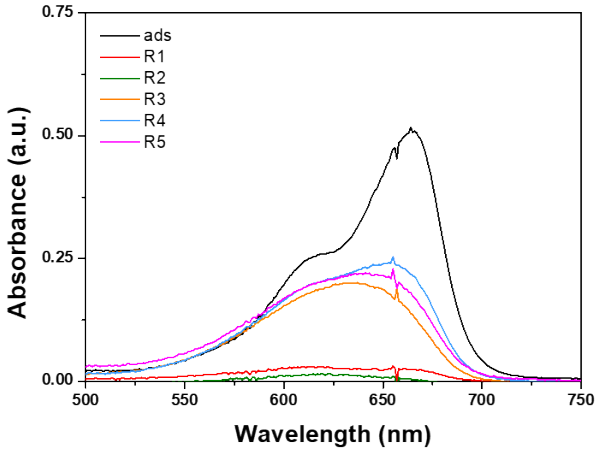

Fig. S20. UV-visible absorption spectra of MB for 5 consecutive photocatalytic runs using **F-TiO$_2$@1CTF** hybrid photocatalyst.

References

1 X. Zheng, S. Meng, J. Chen, J. Wang, J. Xian, Y. Shao, X. Fu and D. Li, *J. Phys. Chem. C*, 2013, **117**, 21263–21273.
2 A. Houas, H. Lachheb, M. Ksibi, E. Elaloui, C. Guillard and J.-M. Herrmann, *Applied Catalysis B: Environmental*, 2001, **31**, 145–157.
3 S. M. Tichapondwa, J. P. Newman and O. Kubheka, *Physics and Chemistry of the Earth, Parts A/B/C*, 2020, **118–119**, 102900.
4 F. Azeez, E. Al-Hetlani, M. Arafa, Y. Abdelmonem, A. A. Nazeer, M. O. Amin and M. Madkour, *Sci Rep*, 2018, **8**, 7104.
5 A. Farghaly, E. Maher, A. Gad and H. El-Bery, *Appl Water Sci*, 2024, **14**, 228.
6 S. S. Muniandy, N. H. Mohd Kaus, Z.-T. Jiang, M. Altarawneh and H. L. Lee, *RSC Adv.*, 2017, **7**, 48083–48094.
7 K. Sonu, S. H. Puttaiah, V. S. Raghavan and S. S. Gorthi, *Environmental Science and Pollution Research*, 2021, **28**, 48742–48753.
8 V. K. Pal, D. Kumar, A. Gupta, P. P. Neelratan, L. P. Purohit, A. Singh, V. Singh, S. Lee, Y. K. Mishra, A. Kaushik and S. K. Sharma, *Diamond and Related Materials*, 2024, **148**, 111435.
9 H. K. Sharma, B. P. Singh and S. K. Sharma, *Hybrid Advances*, 2024, **5**, 100152.
10 M. Shaban, A. M. Ashraf and M. R. Abukhadra, *Sci Rep*, 2018, **8**, 781.